

CHAPTER 2

THE SOLITARY WAVE

Its Celerity, Profile, Internal Velocities and Amplitude Attenuation
in a Horizontal Smooth Channel

James W. Daily
Massachusetts Institute of Technology
Cambridge, Massachusetts
and
Samuel C. Stephan, Jr.
The Carter Oil Company
Tulsa, Oklahoma

INTRODUCTION

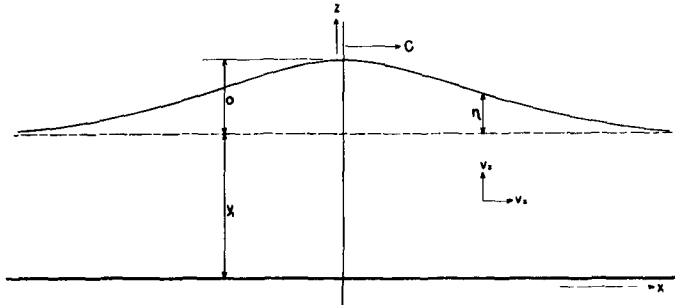
The solitary wave consists of a single elevation of water above the originally undisturbed level as shown in Figure 1. It is translatory, a passing wave causing a definite net horizontal displacement of the liquid. While the characteristics of oscillatory waves depend on wave length as well as wave height and water depth, the solitary wave is apparently described completely by the wave height and water depth so long as attenuation due to friction is unimportant.

It is well known that a close analogy exists between the characteristics of the solitary wave and shallow water waves of long wave length. In recent years this analogy has been used in attempting to predict the characteristics and effects of oscillatory waves moving into shoal water. For this purpose, it has been necessary to use theoretically derived characteristics of the solitary wave, there being very little experimental information beyond J. Scott Russell's (1)(2)* original studies. As a result, there has been a renewed interest in completely determining the properties of the actual wave and checking the rather varied results of the several theoretical analyses.

A summary of the important theoretical analyses for waves moving over a horizontal bottom is given in Table I. The equation for celerity, C , found by Boussinesq (4), Rayleigh (5) and Stoker (14) is the same found empirically by Russell. Keulegan's (12) viscous attenuation equation is for a smooth bottom and agrees with Russell's experimental findings. Munk's (13) work is a restatement of McCowan's analysis using simplifying dimensionless parameters. The coefficients M and N are given graphically in Table I. All the analyses conclude that the wave characteristics are represented by a unique function of the undisturbed depth y_1 and the amplitude-to-depth ratio a/y_1 . Aside from these similarities, the several solutions differ in various respects.

*Numbers in parentheses refer to references at end of this chapter.

COASTAL ENGINEERING

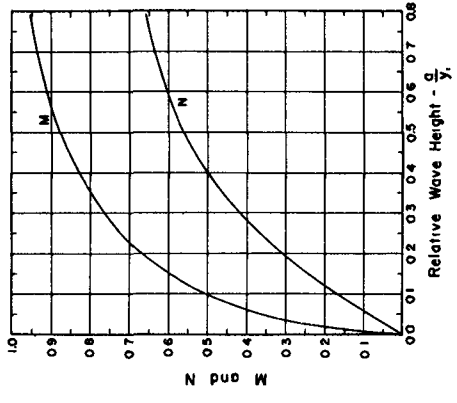


- a - wave amplitude, feet.
- a/y_1 - ratio of wave amplitude to undisturbed depth.
- b - constant coefficients of series in theory by McCowan.
- B - width of wave channel, feet.
- C - wave celerity, ft./sec.
- k - coefficient of series in theory by Davies.
- m - constant coefficient of argument in tangent series by McCowan.
- M - dimensionless coefficient, my_1 , of McCowan's theory as expressed by Munk.
- N - dimensionless coefficient, nb , of McCowan's theory as expressed by Munk.
- P - wetted perimeter of channel cross-section, ft.
- v_x - x - component of instantaneous unsteady motion fluid element velocity, ft./sec.
- v_z - z - component of instantaneous unsteady motion fluid element velocity ft./sec.
- x - horizontal coordinate at channel bottom, with origin at axis of symmetry of wave, feet.
- X - dimensionless horizontal coordinate in theory by McCowan as expressed by Munk, x/y_1 .
- y_1 - undisturbed water depth.
- z - vertical coordinate at axis of symmetry of wave with origin at bottom of channel, feet.
- Z - dimensionless vertical coordinate in theory by McCowan as expressed by Munk z/y_1 .
- z_0 - maximum value of $z = a + y_1$.
- η - $(z - y_1)$, elevation of water surface above undisturbed surface level, $\eta_{\max} = a$.
- ϕ - velocity potential in field of fluid motion.

Fig. 1. Definitions and notations.

THE SOLITARY WAVE

TABLE I

INVESTIGATOR	CELERITY	PROFILE	FLUID ELEMENT VELOCITY	ATTENUATION
St Venant (3)	$C^2 = gy, (1 + \frac{3a}{4y})$			
Boussinesq (4)	$C^2 = gy, (1 + \frac{a}{y})$	$\eta = a \operatorname{sech}^2 \frac{x}{4y}$	$v_x = \frac{a}{\sqrt{y}} \left[\eta - \frac{\eta^2}{4y} + \frac{y^2}{3} - \frac{z^2}{2} \right] \frac{d\eta}{dx}$ $v_z = -\frac{a}{\sqrt{y}} \left[1 - 2\eta + \frac{1}{3} y^2 - \frac{z^2}{2} \right] \frac{d\eta}{dx}$ $U = C \frac{\eta}{2}$	
Rayleigh (5)	$C^2 = gy, (1 + \frac{a}{y})$	$\eta = a \operatorname{sech}^2 \frac{x}{4} \sqrt{\frac{a}{a+y}}$		
McCowan (7)	$C^2 = \frac{g \tan my}{m}$ $C^2 = gy, (1 + \frac{a}{y} + \frac{19a}{12y})$	$\eta = \frac{a}{\tan \frac{mz}{2}} \frac{\sin mz}{\cos mz + \cosh mx}$ $\eta = a \operatorname{sech}^2 \frac{x}{4} \sqrt{\frac{a}{y + \frac{19a}{12}}}$	$v_x = \frac{C m a}{\tan \frac{mz}{2}} \frac{1 + \cos mz \cosh mx}{(\cos mz + \cosh mx)^2}$ $v_z = \frac{C m a}{\tan \frac{mz}{2}} \frac{\sin mz}{(\cos mz + \cosh mx)^2}$	
Stokes (6)	$C^2 = gy, \frac{\tan my}{my}$			
Weinstein (8)	$C^2 = gy, \left[1 + \frac{a}{y} - \frac{2(a^2 y^2)}{20y} \right]$			
Starr (9)	$C^2 = gy, (1 + \frac{3}{2y} \int \frac{a^2 dx}{dx})$			
Davies (10)	$C^2 = gy, \frac{\tan kCy}{kCy}$	$Cx = \phi + \frac{2}{3k} \sin^2 kCy, \frac{\sinh k\phi}{\cosh k\phi + \cos kCy} +$ $Cz = \frac{2}{3k} \sin^2 kCy, \frac{(\cosh k\phi - 1) \tan \frac{1}{2} kCy}{\cosh k\phi + \cos kCy} +$		
Keulegan (12)				$\left(\frac{a}{y}\right)^{\frac{1}{2}} - \left(\frac{a}{y}\right)^{\frac{1}{2}} \frac{1}{12} \left(1 + \frac{2y}{a}\right) \sqrt{\frac{y}{g^2 y^{\frac{3}{2}}}} \frac{x}{y}$
Munk (13)	$C^2 = gy, \frac{\tan M}{M}$	$\eta = Ny, \frac{\sin MZ}{\cos MZ + \cosh MX}$	$v_x = CN \frac{1 + \cos MZ \cosh MX}{(\cos MZ + \cosh MX)^2}$ $v_z = CN \frac{\sin MZ}{(\cos MZ + \cosh MX)^2}$	
Stoker (14)	$C^2 = gy, (1 + \frac{a}{y})$			

Results of theoretical analyses of the solitary wave.

COASTAL ENGINEERING

In general, the theoretical analyses have been based on the assumptions of an infinite wave length, potential motion and a permanent wave form. The solutions have been in the form of various series expansions to different degrees of approximation. In addition, boundary condition assumptions affect the particular solution. An actual solitary wave, on the other hand, has a finite wave length and a non-permanent wave form since from any initial condition viscous attenuation always reduces the amplitude to zero.

Several questions arise then:

- (a) If not permanent, can a wave, nevertheless, be described by a unique function of amplitude to depth ratio?
- (b) To what degree will any existing theory describe an actual wave in which at best the motion is only approximately irrotational?
- (c) Is agreement with theory dependent upon the rate of attenuation, i.e., can different results be expected for different bottom roughness and friction effects?

A program has been underway at M.I.T. under the sponsorship of O.N.R. to provide an experimental foundation for a solidification of the theory and to answer these particular questions. The program has had two phases, studies of waves in a channel with smooth walls and bottom such that friction effects were a minimum, and studies with definite roughnesses. This chapter is a report on the first phase.

SPECIFICATIONS AND EQUIPMENT FOR AN EXPERIMENTAL STUDY

In order to verify any one of the theoretical results, two things are required:

- (a) It is necessary to duplicate as nearly as physically possible the basic boundary conditions inherent in the definition of the wave.
- (b) It is necessary to make measurements with sufficient precision to differentiate between the various theoretical results.

Item (a) concerns the wave channel and generation of the wave. The channel used for these experiments is 13 inches deep, 16-1/2 inches wide and 32 feet long with lucite walls and bottom (Fig. 2). The friction effect which is a minimum with smooth walls and bottom can be varied by coating the bottom with sand or gravel. The width is large with respect to any boundary layer development assuring essentially two-dimensional motion. It has been found universally by investigators that to within the accuracy of experiments made to date, the properties of a wave are indifferent to the mode of generation after the wave has travelled some distance from its origin and providing secondary excitations and disturbances are avoided in the

THE SOLITARY WAVE



Fig. 2. Wave channel with plunger type wave generator installed.

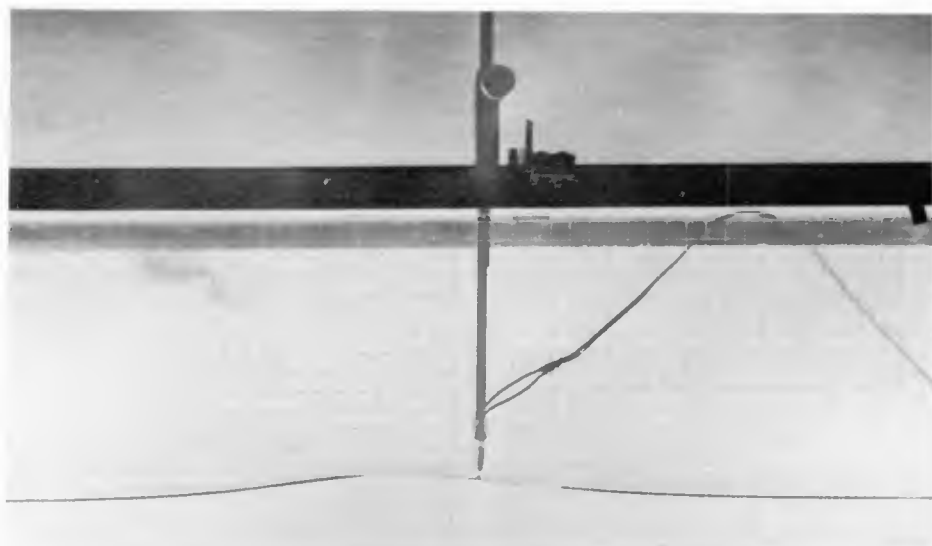


Fig. 3. Solitary wave propagating on 0.2 feet undisturbed depth.

COASTAL ENGINEERING

generation. Because of the limited length of channel, extreme care was taken to generate a "clean" wave which would assume its characteristic shape in a short distance. Two methods were used. In one, the rapid immersion of a plunger displaced a quantity of water equal to the initial wave volume. As the wave surged away from the point of generation, it assumed the characteristic solitary wave form. In the second, more effective method, water in a small reservoir in one end of the channel was released into the channel by raising a sluice gate. This flood of water exerted pressure on a wall, perpendicular to the channel axis and free to move in a horizontal direction, causing it to move as a piston a short distance along the channel. Again the displacement equalled the initial volume of the wave.

The required precision of measurements depends upon the magnitude of differences between expressions for any wave property and upon the actual scale of the experimental waves.

A numerical comparison of the relations in Table I reveals that for the amplitude-to-depth ratio equal to 0.1, the minimum percentage difference between theoretical celerities is about 0.2%. This difference increases rapidly for a/y_1 greater than 0.1. The difference between the two closest theoretical profiles is a maximum of only about 3% of the amplitude when a/y_1 is 0.1. This difference also increases with increasing a/y_1 . Fortunately too, the several profiles vary in such a manner that this extreme precision was not necessary for proper matching to experimental surface curves.

The celerity is determined by timing the wave over a distance of approximately 12 feet. An electronic device triggered by the wave at the beginning and end of the test distance starts and stops an electric timer and simultaneously flashes electronic speed lamps for two photographs of the wave. The travel time can be read from the electric timer to ± 0.001 sec. From photographs, the initial and final positions of the wave axis and hence the travelled distance is established ± 0.005 feet. The resulting accuracy of the celerity measurements is better than $\pm 0.1\%$. However, as the celerity determined is actually the mean celerity for the timing distance of wave travel and as each celerity must be associated with a measured amplitude to be of any value, the accuracy of measurement of the amplitudes becomes the criterion to be considered in evaluating the experimental data. Also, since the amplitude attenuation over this distance is nearly linear and the magnitude decrease is small, it is felt that, within the experimental accuracy of measurement, the mean value of amplitude can be associated with the measured mean celerity.

The photographs are made through a grid inscribed on a sheet of transparent lucite as shown in Figure 3. From enlargements approximately one and one-half natural size, measurements of the profile and amplitude are obtained to within ± 0.001 foot. The undisturbed depth can be measured to within ± 0.0005 foot. Thus the absolute accuracy of amplitude or surface profile elevation measurements is about ± 0.001 foot.

THE SOLITARY WAVE

In the experiments, a maximum depth of about 0.4 feet was used, as this gave sufficient freeboard and provided a good width-to-depth ratio. The minimum depth was set at 0.2 feet principally because of the inability of the generating apparatus to produce waves without secondary disturbances at the very low depths. No amplitudes less than 0.04 foot were used at the 0.4 foot depth and none less than 0.05 foot at the 0.2 foot depth. Thus for these ranges of amplitudes and depths, the resulting combined error in comparing calculated and measured celerities is approximately $\pm 0.3\%$. The resulting error for profile measurements reported here is of the order of $\pm 1.5\%$ of the crest amplitude.

Studies of the motion of the fluid elements are conducted by injecting small droplets of η -butyl thalate and xylene colored red into the water at several depths. By adjusting the specific gravity of the mixture to match that of the water in the channel, the droplets remain suspended in the water and move freely with any motion of the water. Using a 35 mm. movie camera and a stroboscopic flash lamp, photographs at timed intervals are taken of the droplets in their various positions during a wave passage. The positions of the droplets are measured from the frames of the movie film which are projected with a grid superimposed. Knowing the time interval of the frames, the average velocity of the droplets between each position is determined. From several such droplets within the water depth, the velocity distribution is obtained.

WAVE CHARACTERISTICS

PROFILE

Typical experimental profiles selected from the numerous runs are shown in Figures 4 and 5, where points from the photographic records (small circles) are compared with the Boussinesq theoretical profile (solid line). In Figures 4 and 5a the entire experimental range of the amplitude-to-depth ratio, a/y_1 , is represented, while, except for two cases, the undisturbed depth y_1 is nearly constant.

Although no theoretical function was found to represent the wave profile exactly, it was determined that those equations involving the use of the square of the hyperbolic secant more nearly approximated the experimental data than did the others. In particular, the wave profile as determined by Boussinesq (4) gives the most consistent agreement and was used in Figures 4 and 5.

In making a comparison of the experimental profile measurements with the theoretical wave profile as described by Boussinesq's analysis, consistent deviations from the theory are observed as follows. At the higher wave amplitudes for any depth, the experimental profile has a sharper crest with more gentle side slopes and a broader base, while the lower amplitudes exhibit characteristics of an opposite nature, being flatter at the crest with steeper side slopes and a shorter base

COASTAL ENGINEERING

than given by theory. Several profiles are shown in Figure 5b with approximately the same a/y_1 value, but for different values of y_1 . Here a tendency is shown for the base width of a wave propagated in the smaller undisturbed depths to be proportionately longer than a wave at the larger depths when they are compared with the theoretical profiles for the respective a/y_1 values.

Thus, for the amplitudes and depths examined in this investigation, the experimental profile varies systematically about the theoretical profile as described by Boussinesq.

CELERITY

The results of the experimental measurements of wave celerity are shown in Figures 6 and 7. It is seen in Figure 6 that a smooth curve through the experimental data describing the dimensionless relationship between $C/\sqrt{gy_1}$ and a/y_1 falls roughly at a constant angle to the curve representing the relationship $C/\sqrt{gy_1} = \sqrt{1 + a/y_1}$. This latter expression is the theoretical celerity function as derived empirically by Russell (1) and theoretically by Rayleigh (5) and Boussinesq (4) and as a first approximation by later investigators. At the lower a/y_1 values, the experimental points give a celerity that is about 99% of that given by theory with experimental values decreasing to about 97.5% of the theoretical at the highest a/y_1 used in this investigation. Major deviations from a smooth curve occur at low values of a/y_1 , where experimental accuracies are appreciably lower, due to the small magnitudes to be measured.

In Figure 7, a comparison of the absolute experimental celerity values with those as given by the Boussinesq expression is shown. A smooth curve through the experimental data on this plot gives an experimental celerity that is 99.4% of the theoretical at the low celerity values and an experimental celerity that is 98.7% of the theoretical at the high celerity values. For presenting the results of the experimental investigation, the representation in Figure 6 is a more sensitive expression of the celerity relationship.

The equations using higher degrees of approximation obtained by other investigators deviate sufficiently from the equation of the first approximation to be usable with increased accuracy only in restricted ranges. Thus, as is shown in Figure 6, the curves representing the analytical results of McCowan and Weinstein depart radically from the experimental results as a/y_1 is increased. The results of McCowan and Weinstein represent the limiting examples of the equations from the so-called higher approximation. The other analyses result in curves that lie between the latter two curves.

On the basis of the comparison shown in Figure 6, it is felt that the equation of the solitary wave celerity as presented by the first-

THE SOLITARY WAVE

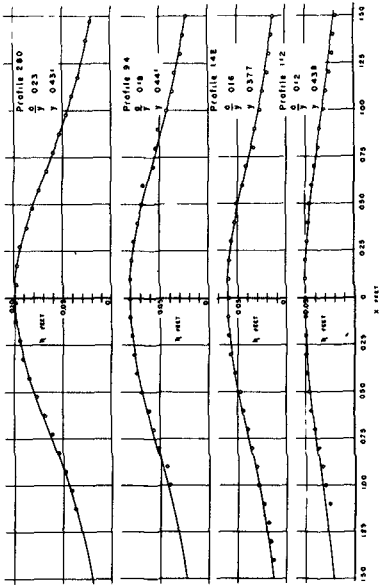
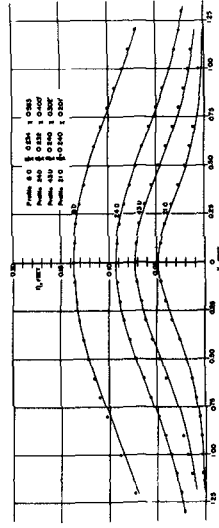


Fig. 4. Experimental profiles (circles) compared with Boussinesq's theoretical profile (solid line).

a. a/y_1 variable at constant depth.



b. a/y_1 constant at variable depth.

Fig. 5. Experimental profiles (circles) compared with Boussinesq's theoretical profile (solid line).

COASTAL ENGINEERING

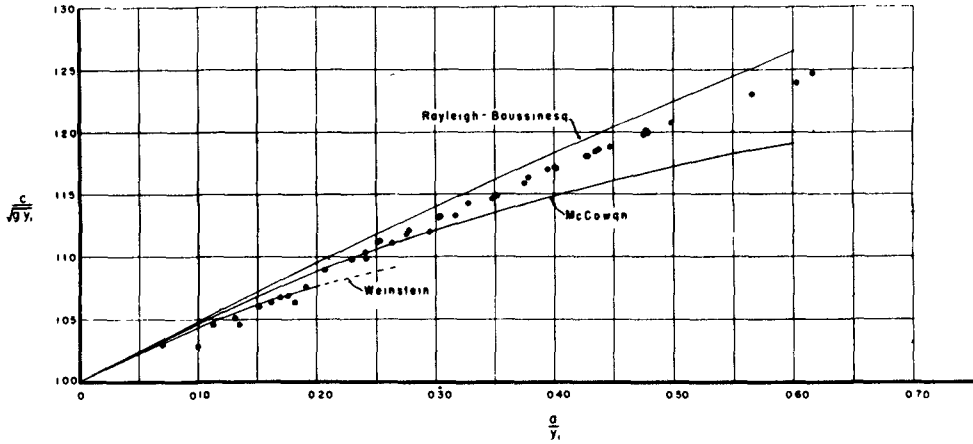


Fig. 6. Dimensionless comparison of experimental celerity data with theoretical celerity curves.

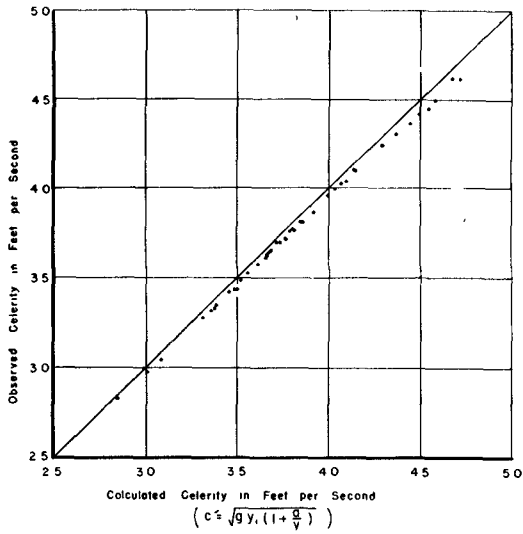


Fig. 7. Measured absolute celerity compared with Rayleigh-Boussinesq values.

THE SOLITARY WAVE

approximation analysis of Rayleigh and Boussinesq is one that will give very close results for practical application to all values of a/y_1 .

FLUID ELEMENT VELOCITY

The motion of suspended droplets was recorded on 35 mm. motion-picture film, using an open shutter and stroboscopic lighting with a flash period of 0.055 seconds. The position of each particle in successive frames was measured and the horizontal and vertical components of the mean velocity between each position were calculated. Typical sets of particle position and velocity component data are shown in Figures 8 and 9. Figure 8 shows the absolute paths of particles at different levels. The effect of the passing wave in producing a mass transport is clearly shown. Figure 9 which shows v_y plotted against v_x , is a useful diagram for correlating the components. It will be noted that there is some irregularity in these derived velocity components. Although the droplet positions were measured from enlargements of about two times natural size, the accuracy of measurement remained at about ± 0.001 feet. With a maximum displacement of the droplets of about 0.05 feet in the time interval of 0.055 seconds, the minimum percentage error obtained was approximately $\pm 2\%$, which became greater as the displacement distances decreased. Since no discontinuities are observed in the motion of the fluid, a continuous smooth relationship must exist between v_x and v_y . The solid curves drawn in Figure 10 represent such a correlation. Working backward then, adjustments of the measured positions of the droplets can be made for a more precise determination of the velocity-space distribution.

Using the correlated results, dimensionless diagrams such as those in Figures 10ab-12ab were prepared showing isovels of fluid elements and corresponding paths of the particles all relative to the wave axis. Additional diagrams appear in Ref. (15). Figures 10b-12b illustrate the apparent paths of the particles for the condition of steady motion. In Figures 10a-12a, the dimensionless isovels are the ratio of the local velocity to the wave celerity, and elevation and horizontal distance are expressed as fractions of the undisturbed depth y_1 . For purposes of comparison, theoretical isovels are shown in Figures 10a-12a using Munk's formulation of McCowan's results (see Table I). In these figures, the heavy solid and dashed curves represent lines of equal vertical velocity and the light curves are lines of equal horizontal velocity. McCowan's results are used because only his analysis leads to explicit expressions for velocity components throughout the field of motion. While several other theoretical investigations of the particle paths and local velocities have been made, all, with this exception, seem to have by-products in the general scheme of analysis giving results for only special conditions. Examples of the latter are surface and bottom element velocities or the mean velocity over a vertical cross section such as determined by Boussinesq.

Examination of the isovel plots in comparison with the correlation diagram shows that the best accuracy of measurement was obtained at the

COASTAL ENGINEERING

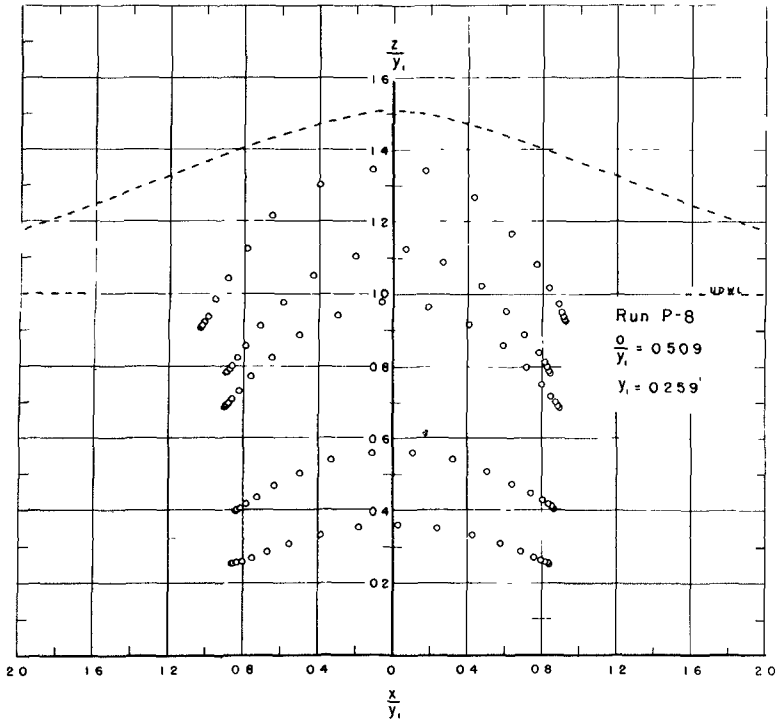


Fig. 8. Absolute paths of suspended droplets shown as they appear to a stationary coordinate system. The dashed wave profile is just for comparison with paths of droplets.

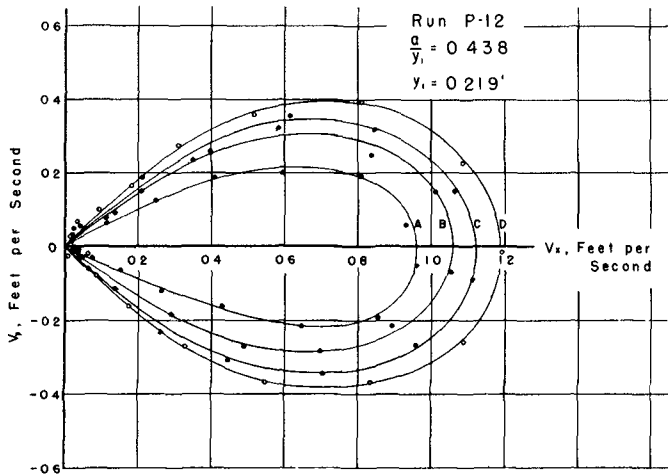


Fig. 9. Illustrating the use of the correlation between the components of fluid velocity to smooth out the irregularities in the experimental data. The solid curve is drawn as a best fit and values of components read from it. The points are the experimental data for four droplets at different elevations.

THE SOLITARY WAVE

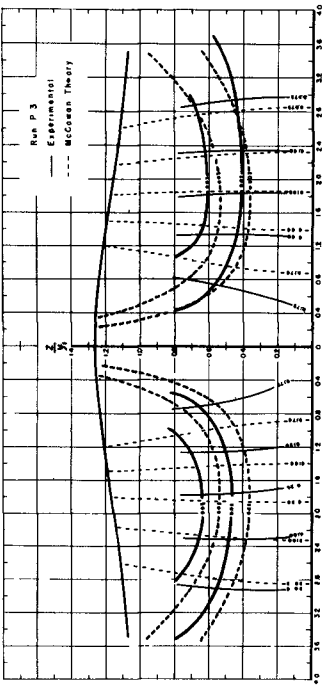


Fig. 10a. Comparison of components of local fluid element velocity according to McCowan with the components determined by experiment. Heavy isovels show equal vertical velocity. Light isovels show equal horizontal velocity. $a/y_1 = 0.265$, $y_1 = 0.345$ feet, $C = 3.709$ ft/sec. Values of isovels are ratios of element velocities to wave celerity.

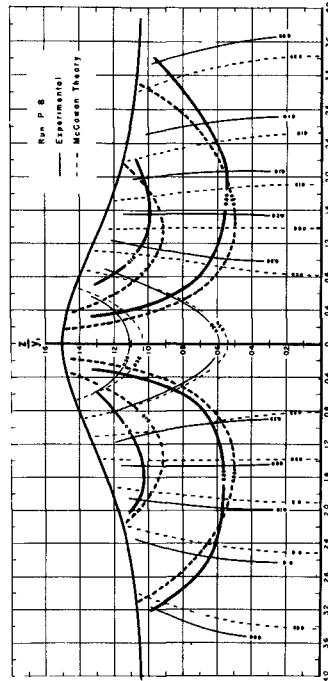


Fig. 11a. Comparison of components of local fluid element velocity according to McCowan with the components determined by experiment. Heavy isovels show equal vertical velocity. Light isovels show equal horizontal velocity. $a/y_1 = 0.259$, $y_1 = 0.259$ feet, $C = 3.502$ ft/sec. Values of iso-

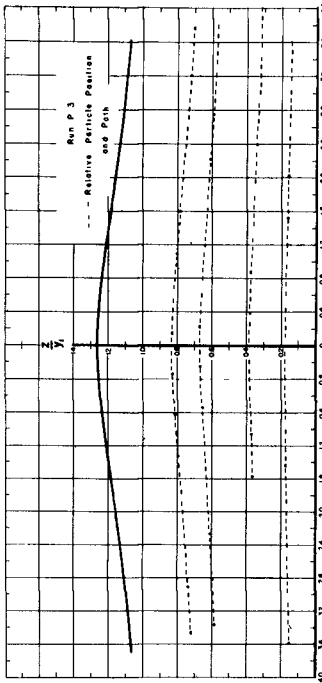


Fig. 10b. Positions of suspended droplets relative to the wave profile and axis at intervals of 0.055 second, illustrating the paths for the condition of steady motion.

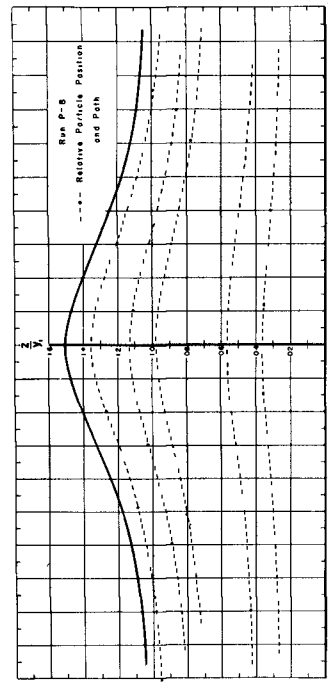


Fig. 11b. Positions of suspended droplets relative to the wave profile and axis at intervals of 0.055 second, illustrating the paths for the condition of steady motion.

COASTAL ENGINEERING

wave axis. Actual observations of the droplet positions were made over a much longer period than is represented by the extent of the isovel plots. However, near the ends of the wave, the irregularities in the measurement became so large relative to the displacement distances that no satisfactory analysis could be made.

As McCowan's results show, a different distribution characterizes each amplitude-to-depth ratio. However, the experimental results otherwise do not agree with McCowan's. Towards the ends of the wave, the theoretical fluid velocity is less than the observed velocity. As the wave axis is approached, the situation becomes reversed, the theoretical values equalling the experimental at approximately the inflection point of the surface curve. These differences are consistent for the range of a/y_1 values investigated and, furthermore, are consistent with the differences between the actual and McCowan's theoretical profile. The latter tends to be more peaked with steeper side slopes above and more gentle side slopes below the point of inflection of the surface curve. Boussinesq's analysis yields the logical conclusion that the rate of increase or decrease of velocities is a function of rate at which the surface profile rises or falls. Assuming this holds the observed trends of actual velocities are logical.

In general, it was observed that the droplets move from an initial position of rest to a final position of rest without any orbital component. However, some exceptions were noted in which a backward component of motion was indicated. This cannot be construed as positive evidence, because of possible secondary influences, such as residual motion in the fluid or disturbances accompanying the main wave. However, there is this indication that the motion of the fluid element in the solitary wave merely represents the extreme limiting condition of the motion observed for wave trains. A more accurate method of measurement of the droplet displacement distances would be required to positively evaluate any such motion.

ATTENUATION

The attenuation of the wave amplitude is determined from photographs of the wave taken at various intervals of travel as it is reflected up and down the length of the channel. Figure 13 shows the results for tests with undisturbed depths of 0.2, 0.3 and 0.4 feet on a smooth channel bottom. The data for each depth is a composite of several runs. With the first experimental run at a given depth having the maximum possible initial amplitude, the subsequent runs were made with each wave amplitude slightly less than the preceding. This was necessary because only twelve passages of the wave could be made without reloading the cameras. By adjusting the origin of the abscissa for each run, a single curve was obtained for each depth.

THE SOLITARY WAVE

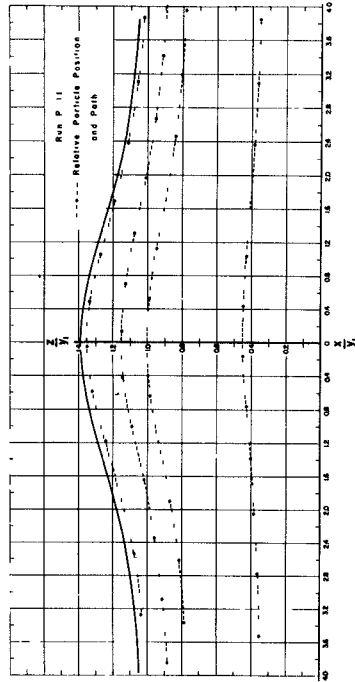


Fig. 12b. Positions of suspended droplets relative to the wave profile and axis at intervals of 0.055 second, illustrating the paths for the condition of steady motion.

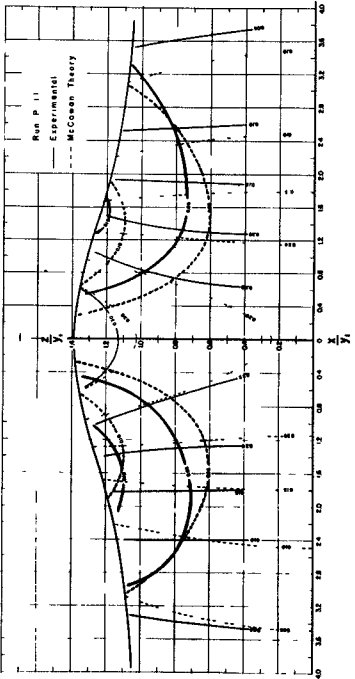


Fig. 12a. Comparison of components of local fluid element velocity according to McCowan with components determined by experiment. Heavy isovels show equal vertical velocity. Light isovels show equal horizontal velocity. $a/y_1 = 0.388$, $y_1 = 0.207$ feet, $C = 3.003$ ft/sec. Values of isovels are ratios of element velocities to wave celerity.

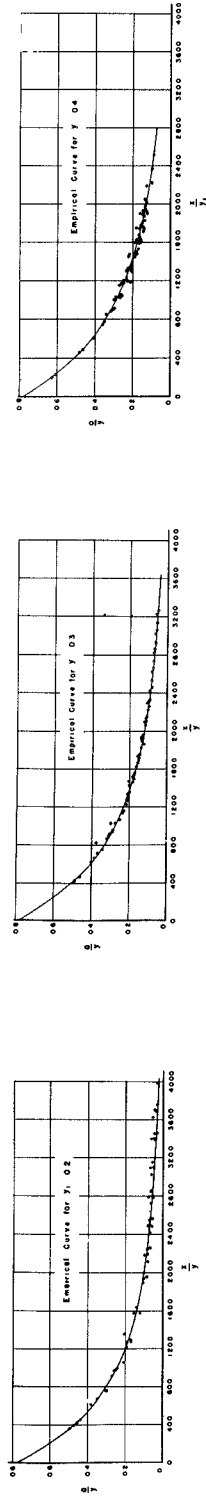


Fig. 13. Attenuation on a smooth bottom. Each empirical curve begins at the arbitrary value $a/y_1 = 0.78$.

COASTAL ENGINEERING

A dimensional analysis gives for the rate of change of amplitude with a smooth bottom

$$\frac{\Delta a}{\Delta x} = \text{const} \times \left(\frac{a}{y_1}\right)^m \left(\frac{\gamma}{g^{1/2} y_1^{3/2}}\right)^q \left(\frac{B}{y_1}\right)^t \left(\frac{P}{y_1}\right)^v$$

where in addition to terms already defined, x = distance along channel, B = channel width, P = wetted perimeter, γ = kinematic viscosity, and m , q , t , v are exponents. Empirically, the data represented in Figure 13 corresponds to $m = 5/4$, $q = 1/2$, $t = -2$, $v = 2$, and the constant = $1/20$, so that on integrating between an initial amplitude a_0 and a we get

$$\left(\frac{a}{y_1}\right)^{-1/4} - \left(\frac{a_0}{y_1}\right)^{-1/4} = \frac{1}{20} \left(1 - \frac{2y_1}{B}\right)^2 \left(\frac{\gamma}{g^{1/2} y_1^{3/2}}\right)^{1/2} \frac{x}{y_1}$$

This gives slightly lower attenuation rates than Keulegan's (12) theoretical equation.

SUMMARY OF OBSERVATIONS

These experiments conducted in a 16-1/2 inch wide horizontal smooth bottomed channel with undisturbed water depths between 0.2 and 0.4 feet give the following:

1. The celerity is adequately described for practical applications by the equation derived empirically by Russell and theoretically by Boussinesq and Rayleigh and given as

$$C = \sqrt{g y_1} \sqrt{1 + \frac{a}{y_1}}$$

The theoretical celerity is approximately 2.5% higher than the experimental value at $a/y_1 = 0.6$ with the difference decreasing as a/y_1 increases. Experimental celerities were determined over the range of a/y_1 from 0.07 to 0.61.

2. The wave profile is closely approximated by the theoretical profile given by Boussinesq as

$$\eta = a \operatorname{sech}^2 \frac{x}{y_1} \sqrt{\frac{3}{4} \frac{a}{y_1}}$$

The experimental profiles were determined over the range of a/y_1 from 0.12 to 0.61. At high a/y_1 , the theoretical profile exhibits a slightly flatter crest than the experimental with the opposite true at low a/y_1 . Best agreement is at $a/y_1 = 0.23$.

3. The experimentally determined fluid element velocity distribution depends upon a/y_1 in manner similar to that predicted by McCowan's

THE SOLITARY WAVE

solution. The differences between the measured and the theoretical values increase with increasing a/y_1 , but are consistent with the differences between the actual and the McCowan profile.

4. The attenuation with a smooth horizontal channel bottom was found to be described by the expression

$$\left(\frac{a}{y_1}\right)^{-1/4} - \left(\frac{a_0}{y_1}\right)^{-1/4} = \frac{1}{20} \left(1 + \frac{2y_1}{B}\right)^2 \left(\frac{\gamma}{g^{1/2} y_1^{3/2}}\right)^{1/2} \frac{x}{y_1}$$

This gives slightly lower attenuation rates than predicted by Keulegan.

REFERENCES

- (1) Russell, J. Scott, "Report of the Committee on Waves", Meeting of the British Association for the Advancement of Science, 1838, p. 417.
- (2) Russell, J. Scott, "Report on Waves", Fourteenth Meeting of the British Association for the Advancement of Science, 1845, p. 311.
- (3) de St. Venant, B., "Theorie du Movement Non Permenent des Eaux, Avec Application aux Cures Rivieres et a l' Introduction des Marees dan leur Lit", Comptes Rendus, Vol. 73, 1871, p. 147.
- (4) Boussinesq, J., "Theorie Des Onde Et Des Remous Qui Se Propagent Le Long D'un Canal Rectangulaire Horizontal, en Communiquant Au Liquide Contenu Dans Ce Canal Des Vitesses Sensiblement Parielles de La Surface Au Fond", Journal of Mathematics, Liouville, France, Vol. 17, 1872, p. 55.
- (5) Rayleigh, Lord, "On Waves", The London, Edinburgh, and Dublin Philosophical Magazine and Journal of Science, Vol. 1, 1876, p. 257.
- (6) Stokes, G. G., "On the Highest Wave of Uniform Propagation", Mathematical and Physical Papers, Vol. 5, 1905, p. 140.
- (7) McCowan, J., "On the Solitary Wave", The London, Edinburgh, and Dublin Philosophical Magazine and Journal of Science, Vol. 32, No. 5, 1891, p. 45.
- (8) Weinstein, A., "Sur La Vitesse De Propagation De L'Onde Solitaire", Comptes Rendus, Accademia del Lincei, Vol. 3, No. 8, 1926, p. 463.
- (9) Starr, V. P., "Momentum and Energy Integrals for Gravity Waves of Finite Height", Journal of Marine Research, Vol. 6, No. 3, 1947, p. 175.
- (10) Davies, T. V., "Gravity Waves of Finite Amplitude", Kings College University of London. To be published.

COASTAL ENGINEERING

- (11) Keulegan, Garbis H., and Patterson, George W., "Mathematical Theory of Irrotational Translation Waves", Journal of Research, National Bureau of Standards, Vol. 24, 1940, p. 47.
- (12) Keulegan, G. H., "Gradual Damping of Solitary Waves", Journal of Research, National Bureau of Standards, Vol. 40, 1948, p. 487.
- (13) Munk, Walter H., "The Solitary Wave Theory and its Application to Surf Problems", Annals of the New York Academy of Science, Vol. 51, 1949, p. 376.
- (14) Stoker, J. J., "Surface Waves in Water of Variable Depth", Quarterly of Applied Mathematics, Vol. 5, No. 1, 1947, p. 1.
- (15) Daily, J. W., and Stephan, S. C., "The Solitary Wave--Its Celerity, Profile, Internal Velocities and Amplitude Attenuation", M.I.T. Hydrodynamics Laboratory Report No. 8, June 1952.